

A Self-adaptive Collaborative Differential Evolution Algorithm for Solving Energy Resource Management Problems in Smart Grids

Haoxiang Qin, Wenlei Bai, Yi Xiang*, Fangqing Liu, Yuyan Han, and Ling Wang

Abstract—Handling energy resource management (ERM) in today’s energy systems is complex and challenging due to uncertainties arising from the high penetration of distributed energy resources. Such penetration introduces various uncertain factors, such as renewable energy, energy storage, and electric vehicles, making it difficult for traditional mathematical methods to find effective solutions. However, Evolutionary Algorithms (EAs) have shown good performance in solving this problem. Therefore, in this paper, a self-adaptive collaborative differential evolution algorithm (SADEA) is proposed to solve the ERM problem under uncertainty. In SADEA, a three-stage adaptive collaboration strategy, includes boundary randomization stage, knowledge-assisted collaboration stage, and range restructuration stage, is used to generate collaborative solutions. The collaborative solutions generated in the above stages will jointly participate in the perturbation of DE strategies to explore promising solutions. In addition, different DE strategies are selected according to count values and random factors. At the end of the algorithm, boundary control, elite selection and retention are used to ensure the legitimacy and robustness of solutions. The proposed SADEA is compared to several state-of-the-art algorithms on a real-world distribution network located in Salamanca, Spain. The results show that SADEA is superior to its competitors in terms of the objective function, ranking index, and convergence. In summary, the proposed algorithm is effective to handle the ERM problem under uncertainty.

Index Terms—Energy resource management, smart grid, uncertainty scheduling, differential evolution, optimization.

I. INTRODUCTION

IN recent years, with the continuous development of technology, the power grid has evolved into an advanced electric grid, namely smart grid (SG) [1]. The SG is the power

This work is partially supported by the National Natural Science Foundation of China under grant numbers 61906069, Natural Science Foundation of Guangdong Province (2022A1515110058), Guangzhou Science and Technology Planning Project (2023A04J1684), and the Natural Science Research Project of Education Department of Guizhou Province (QJJ2023061, QJJ2023012). We would like to thank Instituto Superior de Engenharia do Porto (ISEP) and Universidade Estadual Paulista - Portal (UNESP), organizers of the 2023 Evolutionary Computation in the Energy Domain: Operation and Planning Applications. In addition, we are grateful for the Guangyue Young Scholar Innovation Team of Liaocheng University under grant number LCUGYTD2022-03. (*Corresponding author: Yi Xiang*)

H. X. Qin, Y. Xiang, and F. Q. Liu are with the School of Software Engineering, South China University of Technology, Guangzhou 510006, China (e-mail: 987352978@qq.com; xiangyi@scut.edu.cn; peerfog@scut.edu.cn).

W. L. Bai is with the Oracle America Inc., Austin, TX, and Baylor University, Waco, Texas, USA (e-mail: baiwenlei123@gmail.com).

Y. Y. Han is with the School of Computer Science, Liaocheng University, Liaocheng 252059, China (e-mail: hanyuyan@lcu.cs.com).

L. Wang is with the Department of Automation, Tsinghua University, Beijing 100084, China (e-mail: wangling@tsinghua.edu.cn).

grid that uses advanced commutation technology and control programs, such as demand response (DR), voltage optimization control, fault location, isolation and service restoration. Its main feature is the large penetration of distributed energy resources (DERs). However, DERs (e.g., wind and solar generation) are, by nature, intermittent, which makes it difficult to operate SG reliably and economically [2], [3]. Thus, for embracing DERs, the energy resources management (ERM) system is proposed to automatically negotiate actions, with the goal of achieving a dynamic supply-demand balance [4].

In SG, ERM simply refers to a real-time control system which is used to manage energy resources. It can be modeled as a mixed integer nonlinear problem (MINLP) where profits are to be maximized through control and automation capabilities [5]. To achieve such a goal in real-world scenarios, ERM must interact with various resources under uncertainty, such as electricity market prices, DR procedures, renewable energy generation, energy storage systems (ESSs) and electric vehicles (EVs) [6], [7].

Currently, many studies have made various attempts to tackle the aforementioned uncertainties in resource management. Most of them use traditional mathematical methods, such as robust optimization models [8], [9] and stochastic models [10], [11]. Typically, these models are solved by using deterministic mathematical methods. Nevertheless, traditional mathematical methods face several challenges, including the management of large amounts of resources, high level of accuracy for uncertainty representation, and integration of nonlinear functions (e.g., alternating current power flow and generator quadratic functions) [12]. The above limitations drive researchers to seek for different approaches to tackle this problem, and it has been found that Evolutionary Algorithms (EAs) are capable of effectively solving this problem [13].

Inspired by biological evolutionary mechanisms, EAs adopt operations like crossover, mutation, selection, abandonment, and retention to improve solutions. Well-known EAs include Genetic Algorithms (GA) [14], [15], Differential Evolution (DE) algorithms [16], Particle Swarm Optimization (PSO) algorithms [17], and Iterated Greedy (IG) algorithms [18]–[20]). However, population-based GA, DE, and PSO cannot focus all their efforts on a particular solution during the evolution. The IG algorithm, a single-individual EA, focuses all its efforts on a single solution, which is one of the main reasons for its strong local search ability [21]. However, existing IG algorithms tend to achieve good results in solving discrete problems, and yet not continuous problems such as the ERM

problem under uncertainty. One of the obvious drawbacks is its poor global search ability due to the lack of solution diversity [22]. Therefore, if using a single-individual mechanism, it is necessary to design perturbation strategies that can improve the global search ability of the algorithm. Inspired by [12], we find that the DE strategy is effective in improving the global search ability of the IG algorithm. Therefore, we utilize the single-individual mechanism with the DE strategies, hoping to solve the ERM problem, efficiently.

The major challenges for the ERM problems are summarized as follows.

- Extreme scenarios may endanger the operation or even destroy the aggregator. This requires a risk-based optimization model to protect aggregators from events with low probability and yet high impacts.
- So far, only a few EAs have considered risk-based methodologies when solving ERM under uncertainty. EAs are very subject to the constraints of the ERM. If certain conditions change, the search ability of EAs cannot be fully utilized.
- Population-based EAs may not be able to focus on a promising neighborhood of current solutions, which will distract the computational performance of algorithms and result in a stagnation of the entire evolution. In addition, according to the results in [23], the global search ability of the perturbation strategy also needs to be further improved.

Nevertheless, DE strategies still have many advantages, such as good perturbation and stable convergence. At present, the variants of DE, e.g., HyDE [12] and ReSaDE [24] (won first place in the WCCI (CEC)/ECCO 2022 competition) have been used to solve the uncertain ERM problem and achieved good results. Therefore, this paper designs the methods based on DE strategies. Given the above challenges, our study transforms the population-based DE into a single individual to avoid dispersed search. During the search process, collaborative solutions participate in the evolution by using DE strategies, which improve the local and global search abilities. Based on the above, a Self-Adaptive Collaborative Differential Evolution Algorithm (SADEA) is designed to solve the ERM under uncertainty. Contributions of this paper are summarized as follows.

- To choose the most appropriate DE strategy for a certain stage, a *three-stage adaptive collaboration strategy* is designed. In the first stage, three collaborative solutions are utilized to effectively improve solution diversity. In the second stage, a historical archive is used to explore potentially promising solutions while accelerating the search process. In the third stage, the *range restructuring* prevents solutions from falling into local optimum.
- To improve the local search ability, we use a single-individual mechanism. It allows the algorithm to focus all its efforts on a single solution. Compared to population-based optimization algorithms, it can enable the solution to evolve more quickly. Meanwhile, it can reduce the tedious steps, making it suitable for power dispatch in various scenarios.

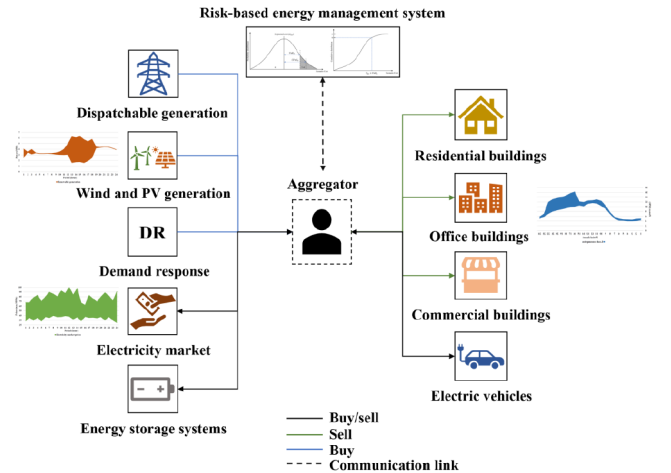


Fig. 1. The ERM problem [25]

- To overcome the weak global search abilities of single-individual EAs, three DE strategies are proposed. The proposed DE strategies significantly increase the diversity of solutions and prevent them from falling into local optimum.

The remainder of this paper is organized as follows. Section II introduces the related work of the ERM problem. The definitions of the problem are given in Section III. Section IV provides a case study of the distribution network, which is a real-world problem to be addressed in this paper. Section V lists details of SADEA. In Section VI, the results show that the proposed algorithm performs better than the state-of-the-art algorithms in solving the ERM problem. The conclusion and future work are given in Section VII.

II. RELATED WORK

In this section, the related work will be divided into two categories: A) Risk-based methodologies, B) EAs-based methodologies.

A. Risk-based Methodologies

Risk-based methodologies have been commonly used in electrical systems to reduce natural disasters or utility outages [26]–[28]. The emergence of extreme scenarios can have a huge impact on the management of electric network operators [29]. Recently, several studies have used risk-based methodologies for aggregators, such as wind power generation [30], conventional hydropower [31], and the uncertainty of micro-grid planning [32]. The work in [33] considered the uncertainty of load and pool market prices, and proposed a risk-based approach to achieve equal cost in an uncertain scenario. This approach increases the retailers' cost but reduces the risk to almost zero. In other words, although the cost increases to a certain extent, it is still worthwhile to reduce the risk to zero for extreme scenarios.

In recent years, risk-based measurement mechanisms such as value-at-risk (VaR_α) have been proposed. However, VaR_α can only measure risk when the expected cost does not exceed the confidence level α for all scenarios. On the contrary,

conditional VaR_α ($CVaR_\alpha$) allows measurement of risk beyond confidence level scenarios [34], [35]. It shows that, by introducing $CVaR_\alpha$, the impact of extreme scenarios will be minimized. Therefore, in this paper, both VaR_α and $CVaR_\alpha$ risk assessment parameters are considered to protect the aggregator. Fig. 1 gives the energy resource Buy/Sell in ERM, and the communication link to the aggregator [25]. The final optimization objective is to maximize the profit, or, to minimize the difference between operational costs (OC) and incomes (In) in each scenario, which takes into account penalty values and risk assessment parameters.

B. EAs Utilized to Solve the Uncertainty ERM

In EAs, CUMDANCauchy [36] generates new individuals not only by sampling from the learned distribution but also by using the individual neighborhoods in a ring cell structure. It achieves better performance compared to variants of PSO or variable neighborhood search algorithms [37]–[39]. In [23], the Cooperative Co-evolution Strategies with Time-dependent Grouping (CCSTG), inspired by cooperative co-evolution frameworks, groups the decision variables into subcomponents. It generates new individuals from the univariate marginal distribution in the subpopulation. Population regeneration star-guided optimization (Presto) (which won the PES-GM/CEC/GECCO 2021 competition) [23] is inspired by PSO and DE algorithms and seeks to increase the diversity of solutions. Hybrid-Adaptive Differential Evolution (HyDE) algorithm [12] uses multiple individuals for a series of evolutions, and although it increases the diversity of solutions, to a certain extent, it sacrifices local search ability. In addition, after one evolution, only improved solutions replace the original ones, while unimproved solutions continue to participate in the next evolution. Therefore, the increase of the solution diversity is limited, and evaluations on multiple solutions will disperse the algorithm's search ability. In addition, the aforementioned EAs do not consider risk-based methodologies.

Restart-assisted Self-adaptive Differential Evolution (ReSaDE) algorithm, which won the first place in the WCCI (CEC)/ECCO 2022 competition [24], divides the variables into four different groups based on their bounded upper and lower bounds and improves them separately. Although this algorithm is tested in ERM with risk assessment parameters, it has several limitations. For example, the grouping is subject to the range of variables. It may lead to performance degradation and scalability issues. In addition, it is difficult to transplant due to its complex structure and strong dependence on problems. Therefore, this paper proposes SADEA to fill these gaps. Compared with ReSaDE, SADEA has a simpler structure, making it easier to solve other similar problems.

III. PROBLEM DESCRIPTION

Risk-based ERM under uncertainty is formulated as a MINLP where the objective for the aggregator is to generate a day-ahead energy schedule for DERs, EVs, ESSs and DR to maximize the expected profits, subject to constraints such as resource limits, energy balance [40]. To protect aggregators from impacts caused by uncertainty, the risk assessment

parameters VaR_α and $CVaR_\alpha$ are introduced. In general, VaR_α deals with the scenarios where events with a high probability of occurrence but a reasonably small effects (such as small error in renewable forecast). $CVaR_\alpha$ considers events with a low probability, but have high impacts (such as hurricanes, thunderstorms, and errors in the forecast).

In this section, the ERM problem will be divided into three parts to illustrate: A) risk-based ERM and fitness function, B) scenario generation, and C) encoding of the solution.

A. Risk-based ERM and Fitness Function

Due to space limitations, the notation of the ERM problem has been included in the supplementary material. Readers can refer to the original literature [35] or the supplementary material for details.

As shown in [35], the risk-neutral strategy considers the uncertain behavior of renewable energy generation, electric vehicles, market prices, load consumption, etc. These stochastic behaviors are considered using various methods that account for different scenarios and their associated probabilities of occurrence. When a risk is not taken into account, the aggregator formulates its schedule based on an expected scenario. In this case, the cost and the objective function (OF) values are based on the expected cost, which is formulated as follows:

$$Z_s^{tot} = Z_s^{OC} - Z_s^{In} + P_s \quad (1)$$

$$Z_s^{Ex} = \sum_{s=1}^{N_s} (\rho_s \cdot Z_s^{tot}) \quad (2)$$

where Z_s^{tot} is the total OF value of each scenario s ; Z_s^{OC} represents the operational costs; Z_s^{In} represents the income and P_s indicates the penalty for bound violations. In Equation (2), Z_s^{Ex} indicates the expected OF; ρ_s denotes the probability of the corresponding scenario s , and N_s denotes the total number of scenarios.

Risk-aversion strategies consider the risks associated with uncertainty. In $(1-\alpha)\%$ of the scenarios with the highest costs, $CVaR_\alpha$ is an additional cost added to Z_s^{Ex} . Its calculation is as follows.

$$CVaR_\alpha(Z_s^{tot}) = VaR_\alpha(Z_s^{tot}) + \frac{1}{1-\alpha} \sum_{s=1}^{N_s} (\rho_s \cdot \varphi) \quad (3)$$

where:

$$\varphi = \begin{cases} Z_s^{tot} - Z_s^{Ex} - VaR_\alpha(Z_s^{tot}), & Z_s^{tot} \geq Z_s^{Ex} + VaR_\alpha(Z_s^{tot}) \\ 0, & \text{otherwise} \end{cases} \quad (4)$$

$$VaR_\alpha(Z_s^{tot}) = z\text{-score}(\alpha) \cdot std(Z_s^{tot}) \quad (5)$$

When the total costs of scenario s exceed the sum of expected costs and Var , φ indicates the cost in the worst scenarios. Otherwise, the value of φ equals 0. In addition, the z-score is calculated using the `norminv()` function in MATLAB with $\alpha = 95\%$. $std()$ represents the standard deviation function. Considering the parameter $CVaR_\alpha$, the

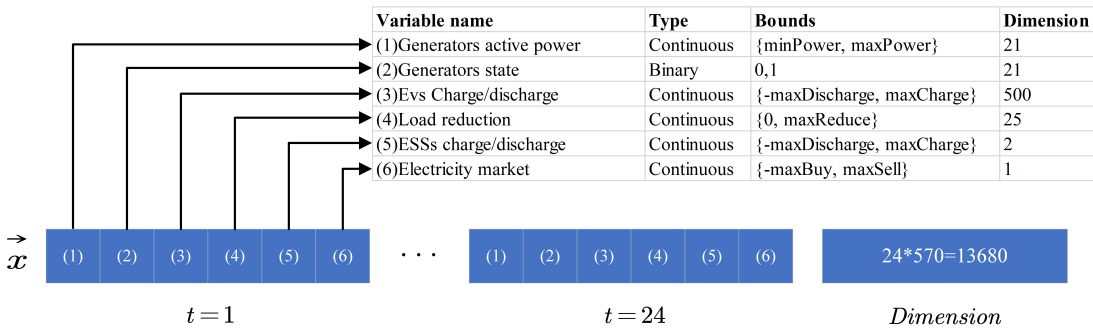


Fig. 2. Solution encoding

value of the OF for this ERM problem varies with the degree of risk aversion considered. The calculation formula for OF is shown as follows.

$$OF = Z_s^{Ex} + \beta \cdot CVaR_\alpha (Z_s^{tot}) \quad (6)$$

where the parameter β denotes the percentage of risk aversion and takes values from 0 to 1. When β takes the value of 0, OF value is merely equal to the expected cost and it's a risk-neutral strategy. Conversely, when β takes the value of 1, the strategy is 100% risk averse to provide the safest solution in the worst extreme scenarios. According to [35], this paper also sets the value of β to 1. In addition, details on different constraints in the ERM problem can also be found in the above literature.

B. Scenario Generation

In the ERM problem, the aggregator needs to handle the uncertainty of multiple resources, such as renewable energy generation, market prices, electric vehicle charging, and load demands. Due to the stochastic nature of the above resources, it is almost impossible to find an exact or perfect solution. Therefore, this paper uses Monte Carlo Simulation (MCS) method [3] to solve the uncertainty of this problem through scenario-based optimization techniques. First, MCS is used to generate a large number of scenarios, and the probability distribution function of the prediction error is:

$$x_s = x^{forecasted}(t) + x^{error,s}(t) \quad (7)$$

where $x^{forecasted}(t)$ indicates the mean forecasted value in each instant t , $x^{error,s}(t)$ represents the value of the error, which concerns each scenario s along with a normal distribution function having zero-mean noise and standard deviation σ , i.e., $N(0, \sigma)$.

After a large-scale scenario generation, a scenario reduction strategy is used to reduce the number of scenarios. Generally, a larger number of scenarios imply higher accuracy, but also higher memory and time. Therefore, it is necessary to apply scenario-reduction strategies to eliminate scenarios with a low probability of occurrence. This is achieved by grouping statistically similar scenarios and reducing the number of scenarios. Similarly, the number of constraints is reduced. Details of this strategy can be found in [41].

C. Encoding of a Solution

This section describes the encoding method of solutions. It is known that depending on the problem characteristics, information is encoded into a solution with different dimensions to measure their performance. Undoubtedly, the information contained in the solution is related to resources, including generator active power, generator's state, and EVs charge/discharge. Fig. 2 shows the encoding of a solution, in which all variables should be between the minimum and maximum values. Except for the state of the generator (represented

by the binary state, where 1 indicates a connection to the SG and 0 indicates no connection), all variables are continuous and changed according to the specified boundaries. There are 24 periods in a solution. In each period, there are 570 sequentially repeated variables. Thus, the total number of variables in one solution is $24 \times 570 = 13680$, with 21 binary variables indicating the generator's state, 21 continuous variables constituting the generator's active power, and 500 continuous variables representing EVs charge/discharge. Load reduction uses 25-dimension continuous variables to represent its situation. The dimension number of the ESSs charge/discharge and electricity market is 2 and 1, respectively. It should be noted that DR is only assumed to be load reduction. For electricity market variables, assume that positive values are electricity sold in the market and negative values are electricity purchased.

IV. CASE STUDY

In our case study, the smart city medium voltage (MV) and distribution network (DN) located in the BISITE Laboratory in Salamanca, Spain is selected [42]. In this DN, there is a 30 megavolt-ampere (MVA) substation, 15 DG units (13 photovoltaic power plants and 2 wind farms), and four 1 MVAr capacitor banks on bus 1 (these capacitor banks are not included in this problem because reactive power is not considered). In terms of consumption, the DN has 25 different loads, consisting of office buildings, residences, shopping centers, fire stations, and hospitals. In addition, the high penetration of EVs and renewable energy sources are considered in this case study. Smart city has seven charging stations to charge EVs, with a 50kW fast charging station at each connection point and four 7.2 kW slow charging stations. Fig. 3 shows the 13-bus 30 kV single-line diagram.

First, 5,000 scenarios are generated, and are subsequently reduced to 150 scenarios using the GAMS/SCENRED [25] technique. Further, it is reduced to 15 scenarios to save computational time. Aggregators must manage various resources and meet consumption by purchasing electricity from external suppliers and purchasing/selling energy in the market. Table I considers the energy resource data related to the aggregator of the previous day's formula in extreme scenarios. Noteworthy, m.u. means monetary unit.

To solve the aggregator energy resource management problem, we propose SADEA. Details of its implementation will be introduced in the next section.

V. METHODOLOGY

Inspired by IG and DE algorithms, the proposed SADEA incorporates a single individual mechanism as well as DE strategies. With these strategies, more precise adjustments can be made to the variables (e.g., renewable energy generation, energy storage, electric vehicle charging and discharging). This improves the algorithm's global and local search abilities, and effectively reduces the cost of aggregators. In addition, SADEA uses a *boundary control strategy* to ensure the legitimacy of the solution. Most importantly, the proposed

TABLE I
ENERGY RESOURCE DATA [35]

Energy Resources	Prices (m.u./MWh)	Capacity (MW)	Forecasted (MW)	Units
	min-max	min-max	min-max	
Wind	29-29		0.00-0.81	2
Photovoltaic	31-31		0.30-3.07	13
External supplier	50-90	0.00-30.00		1
ESSs	Charge Discharge	110-110 60-60	0.00-1.25 0.00-1.25	2
EVs	Charge Discharge	0-0 60-60	0.01-0.05 0.01-0.05	500
Demand response	Load reduction	100-100	0.00-1.21	25
Load	0-0		0.01-2.38	25
Electricity Market	44.78-156.91			1

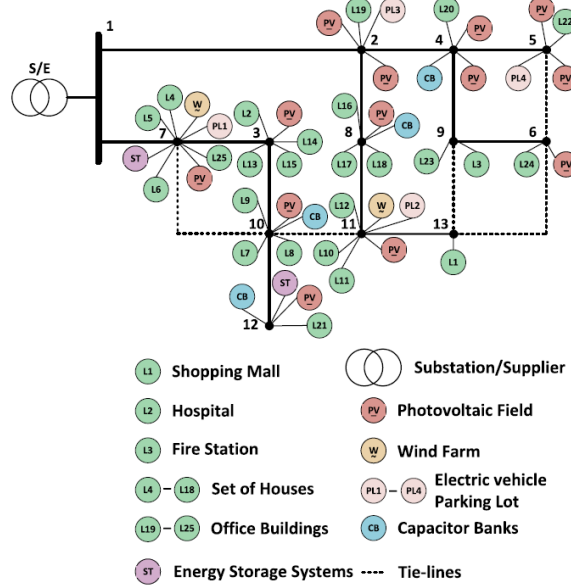


Fig. 3. Single-line diagram of the 13-bus 30-kV DN [42]

algorithm is able to overcome the difficulties of uncertainty and variability in the ERM problem and find effective solutions in extreme scenarios.

A. Framework of the Proposed Algorithm

The framework of the proposed SADEA is outlined in Algorithm 1. We first explain the notations used. G represents the total number of generations, or the termination condition; $\mathbf{F} = \{F_1, F_2, F_3\}$ and F_CR are self-adaptive control parameters (used in DE), which take values between 0 and 1. $\mathbf{x}_c = [x_{c,1}, x_{c,2}, \dots, x_{c,D}]$, where D represents the number of dimensions, denotes the current solution; \mathbf{x}_{best} denotes the obtained global optimal solution, and \mathbf{x}_{new} is a new solution. ϑ , an archive with size Ex_count (a parameter), records solutions that have been successfully updated in the previous generations.

Lines 1-5 in Algorithm 1 aim at initializing \mathbf{x}_c , \mathbf{x}_{best} , ϑ and some internal variables. More specifically, according to Line 1, only one initial solution is used, and values of all its variables are randomly generated between minimum and maximum boundaries. This is achieved by the function *BoundaryRandomization()*. After obtaining \mathbf{x}_c , its OF value is calculated by $f()$ (see Equation (6)), and assigned to OF_{best} . $\vartheta \leftarrow zeros(2, D)$ means to generate an archive of historical data with 2 solutions (according to the experiment in Section VI, we suggest setting the size of ϑ to 2). As

Algorithm 1 The framework of SADEA

Input: self-adaptive control parameters \mathbf{F} , F_CR , the total number of generations G
Output: OF_{best}
Begin:
*/*Initialization*/*
1: $\mathbf{x}_c \leftarrow BoundaryRandomization(1, D);$
2: $\mathbf{x}_{best} \leftarrow \mathbf{x}_c;$
3: $OF_{best} \leftarrow f(\mathbf{x}_c);$
4: $\vartheta \leftarrow zeros(2, D);$
5: $gen = 1, e = 0, count = 0;$
*/*Evolution*/*
6: **while** $gen \leq G$ **do**
7: $\{\mathbf{F}', F_CR'\} \leftarrow jDE(\mathbf{F}, F_CR);$
*/*TSAC(): Three-stage adaptive collaboration strategy*/*
8: $\mathbf{x}_{new} \leftarrow TSAC(\mathbf{F}', F_CR', \vartheta, \mathbf{x}_c, \mathbf{x}_{best}, count);$
9: $OF_{current} \leftarrow f(\mathbf{x}_{new});$
*/*Elite Selection and Retention*/*
10: **if** $OF_{current} < OF_{best}$ **then**
11: $OF_{best} \leftarrow OF_{current};$
12: $\mathbf{x}_c \leftarrow \mathbf{x}_{new};$
13: $\mathbf{x}_{best} \leftarrow \mathbf{x}_c;$
14: $count = 0;$
15: **if** $e < Ex_count$ **then**
16: Put the solution into ϑ ;
17: $e = e + 1;$
18: **else**
19: Use this solution \mathbf{x}_{new} to replace the worst one
in ϑ ;
20: **end if**
21: **else**
22: $count = count + 1;$
23: **end if**
24: $gen = gen + 1;$
25: **end while**
End

seen in Lines 7-8, *jDE* is used to adjust parameters \mathbf{F} and F_CR , then, the *three-stage adaptive collaboration strategy (TSAC)* is used to obtain collaborative solutions based on the adjusted parameters \mathbf{F}' and F_CR' . As shown in Lines 10-24, *elite selection and retention* will be executed. If the current solution is better than the global optimal solution, the current solution will replace it, and ϑ will be updated. If the current solution is inferior to the global optimal solution, no operation will be taken, but the value of *count_1* will be increased by 1.

Algorithm 2 jDE

```

Input:  $\mathbf{F}$ ,  $F\_CR$ 
Output:  $\mathbf{F}'$ ,  $F\_CR'$ 
Begin:
1:  $\mathbf{F}' = \begin{cases} \mathbf{F}_{lower} + rand_1 \cdot \mathbf{F}_{upper}, & \text{if } rand_2 < \tau_1 \\ \mathbf{F}, & \text{otherwise} \end{cases};$ 
2:  $F\_CR' = \begin{cases} rand_3, & \text{if } rand_4 < \tau_2 \\ F\_CR, & \text{otherwise} \end{cases};$ 
End

```

B. Self-adaptive Adjustment Strategy

The self-adaptive adjustment strategy removes the need for parameter adjustment and usually shows good performance for different types of problems. As a useful self-adaptive adjustment strategy, *jDE* was proposed in [16] and successfully applied in [12]. Results demonstrate that adjusting parameters is conducive to find promising solutions. Therefore, this paper uses *jDE* as the parameter-tuning method. In each generation, the calculation of \mathbf{F} and F_CR is shown in Algorithm 2.

In the *jDE* strategy, $rand_j$, $j \in \{1, 2, 3, 4\}$ are generated uniformly at random in the range [0,1]. τ_1 and τ_2 are probability factors. \mathbf{F}_{lower} and \mathbf{F}_{upper} represent the low and upper boundary vectors of \mathbf{F} , respectively. In this paper, the same parameter settings as in [16] are used, i.e., $\tau_1 = \tau_2 = 0.1$. All values in \mathbf{F}_{lower} , \mathbf{F}_{upper} are set to 0.1 and 0.9, respectively.

C. Three-stage Adaptive Collaboration Strategy

In the ERM problem under uncertainty, each variable value in the solution directly affects the final profit. Therefore, how to perturb these variables is important. The SADEA is designed based on DE strategies, which are used to perturb the current solution. The quality of the collaborative solutions, as part of the co-evolution, will have a large impact on the subsequent evolutions. However, in many existing EAs, the perturbation of the solution is not satisfactory. As a result, the collaboration to the current solution may not achieve the desired effect. Therefore, in this paper, we use a single-individual mechanism, which has strong local search ability (demonstrated in [43], [44]), and combine it with DE strategies to improve the effect of SADEA on the perturbation of variable values.

Algorithm 3 gives details of the *three-stage adaptive collaboration strategy*. Note that in the algorithm, \mathbf{x}_c , \mathbf{x}_{r1} , \mathbf{x}_{r2} , and \mathbf{x}_{r3} denote the current and three other collaborative solutions, respectively; $minbound$ and $maxbound$ are boundaries composed of the minimum and maximum values of all variables. Three different DE strategies are designed to perturb the current solution to generate a new solution. The details of the DE strategies are given in Equations (8)-(10).

DE/target-to-minimum boundary best strategy:

$$\mathbf{x}_{new} = F_3 (\mathbf{x}_{r1} + \mathbf{x}_{r3} - 2\mathbf{x}_{r2}) + minbound \cdot (1 - F_1) \quad (8)$$

DE/target-to-perturbed best/I:

$$\mathbf{x}_{new} = F_1 (\mathbf{x}_{best} (F_2 + rand(D)) - \mathbf{x}_c) + \mathbf{x}_c + F_3 (\mathbf{x}_{r1} - \mathbf{x}_{r2}) \quad (9)$$

DE/target-to-perturbed best/2:

$$\mathbf{x}_{new} = F_1 (\mathbf{x}_{best} (F_2 + rand(D)) - \mathbf{x}_c) + \mathbf{x}_c + F_3 (\mathbf{x}_{r1} + \mathbf{x}_{r3} - 2\mathbf{x}_{r2}) \quad (10)$$

As shown in above equations, DE strategies generate a new solution \mathbf{x}_{new} by perturbing \mathbf{x}_{r1} , \mathbf{x}_{r2} and \mathbf{x}_{r3} . F_1 , F_2 , and F_3 are three factors obtained from the *jDE* strategy, which are included in \mathbf{F} and take values in the range [0,1]; \mathbf{x}_{new} is the new solution. $rand(D)$ represents a D -dimensional random vector whose data is all in the range [0,1]; \mathbf{x}_{best} and \mathbf{F} are involved in the perturbation of variables in the solution \mathbf{x}_c ; As shown in Algorithm 3, the related counting parameters *count_1* and *count_2* are suggested to set to 6 and 7, respectively (see the experiment in Section VI). In addition, R is a pre-set fixed value in [0,1].

Algorithm 3 Three-stage adaptive collaboration strategy

```

Input:  $\mathbf{F}'$ ,  $F\_CR'$ , the size of the historical archive  $\vartheta$ , the current solution  $\mathbf{x}_c$ , the best solution  $\mathbf{x}_{best}$ , count
Output:  $\mathbf{x}_{new}$ 
Begin:
    $\mathbf{F} = \mathbf{F}'$ ,  $F\_CR = F\_CR'$ ;
   /*boundary randomization stage*/
1: if count < count_1 then
2:     Randomly generate collaborative solutions  $\mathbf{x}_{r1}$ ,  $\mathbf{x}_{r2}$ , and  $\mathbf{x}_{r3}$ .
3:     if  $rand() \leq R$  then
4:         Generate  $\mathbf{x}_{new}$  using Eq.(9).
5:     else
6:         Generate  $\mathbf{x}_{new}$  using Eq.(10).
7:     end if
   /*knowledge-assisted collaboration stage*/
8: else if count_1 ≤ count < 11 then
9:     Permute randomly the solutions in  $\vartheta$ , and assign the first three solutions to  $\mathbf{x}_{r1}$ ,  $\mathbf{x}_{r2}$ , and  $\mathbf{x}_{r3}$ , respectively. If the size of  $\vartheta$  is less than 3, then  $\mathbf{x}_{r3} = \mathbf{0}$ .
10:    if count ≥ count_2 then
11:      Generate  $\mathbf{x}_{new}$  using Eq.(8).
12:    else
13:      if  $rand() \leq R$  then
14:         Generate  $\mathbf{x}_{new}$  using Eq.(9).
15:      else
16:         Generate  $\mathbf{x}_{new}$  using Eq.(10).
17:      end if
18:    end if
   /*range restructuration stage*/
19: else
20:     Calculate the difference between maxbound and minbound, the range is obtained, and then  $\mathbf{x}_r = (\mathbf{range}/2 \cdot (i-1)) + minbound$ ,  $i = 1, 2, 3$ .
21:     Generate  $\mathbf{x}_{new}$  using Eq.(8).
22: end if
   /*Crossover*/
23: v =  $rand(D) < F\_CR$ ;
24: Generate  $\mathbf{v}'$  according to the v;
25:  $\mathbf{x}_{new} = \mathbf{v}' \cdot \mathbf{x}_c + \mathbf{v} \cdot \mathbf{x}_{new}$ ;
26:  $\mathbf{x}_{new} \leftarrow BoundaryControl(\mathbf{x}_{new})$ ;
End

```

Fig. 4 shows the DE strategies used in different stages with different colors. In the *boundary randomization stage* of SADEA

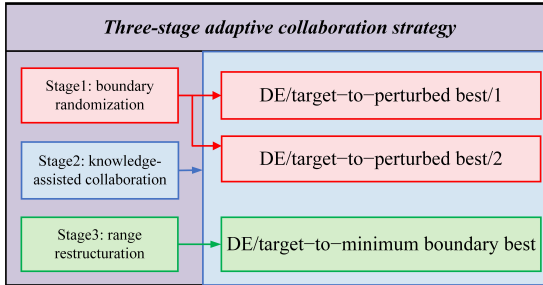


Fig. 4. Illustration of *three-stage adaptive collaboration strategy*

(Algorithm 3, Lines 2-7), first, three random solutions are generated randomly. Then, they are used by *DE/target-to-perturbed best/1* and *2* strategies to perturb the current solution (red rectangular area). When several invalid evolutions occur in the *boundary randomization stage*, it moves to the next stage. In the *knowledge-assisted collaboration stage* (Algorithm 3, Lines 9-18), successfully updated solutions from recent generations are stored into ϑ . Then, *DE/target-to-perturbed best/1* and *2* and *DE/target-to-minimum boundary best* strategies use \mathbf{x}_{r1} , \mathbf{x}_{r2} , and \mathbf{x}_{r3} to further enhance the local search of SADEA, and find promising solutions in the neighborhood of the current solution (blue rectangular area). The purpose of this design is to maintain a certain balance between global search and local search abilities, and not to completely improve the performance of one side at the expense of the other. In the *range restructuration stage* (Algorithm 3, Lines 20-21), *DE/target-to-minimum boundary best* is used to reduce the number of expensive calculations and the number of quality evaluations (green rectangular area). In the *Crossover* (Algorithm 3, Lines 23-25), the operation of generating random solutions is inspired by [12], [45]. \mathbf{v} and \mathbf{v}' are vectors composed of 0 and 1, and the pair of vectors are reciprocal. If the value of certain variable in \mathbf{v} is 1, the value of the corresponding variable in \mathbf{v}' is 0, and vice versa.

D. Boundary Control Strategy

Ensuring the legality and correctness of the obtained solution is an extremely important aspect. In this paper, after the perturbation of DE strategies, variables in the solution are changed. However, some values may exceed the minimum or maximum bounds during the evolution. Obviously, this is not in accordance with the constraints of the ERM. In this case, it is necessary to use the *boundary control strategy* (Algorithm 3, Line 26) to contain the out-of-bounds variables within a reasonable range. This is a simple and effective strategy, which is also used in HyDE [12]. If variable values are greater than the maximum boundary values, maximum boundary values are assigned to these variables. If the variable values are less than the minimum boundary values, minimum boundary values are used to replace these values.

VI. EXPERIMENTAL RESULTS AND ANALYSIS

In this section, the effectiveness of SADEA is to be verified through the following experiments: parameter sensitivity study of SADEA, performance validation of the proposed strategies, and comparison with the state-of-the-art algorithms. In these experiments, all algorithms are coded in Matlab 2020 and performed on a 2.60 GHz Pentium processor, Intel Core i7 under the Windows 11 operating system. The line and violin charts are drawn by Origin; the convergence curve is drawn by Matlab, and other statistical charts are plotted using Excel. The details can be found in the following subsections.

A. Design of the Experiments

In our experiment, SADEA, along with its variants and peer algorithms, is executed with 20 independent runs. In each

run, 15 different scenarios are integrated into a problem black box (the requirements for testing can be found on the website: <http://www.gecad.isept.ipp.pt/ERM-competitions/2023-2/>). When conducting experiments with peer algorithms, we choose two termination conditions, i.e., $G = 3,000$ and $G = 5,000$. The reason is to check the stability and robustness of the algorithms. All parameters and strategies are the same as those used in the original paper or competition. In addition, the RI is used as the performance metric. It is obtained by calculating the average value of N independent runs. A smaller RI value indicates a better algorithm. The calculation formula of RI is shown below:

$$RI = \frac{1}{N} \cdot \sum_{i=1}^N OF_i \quad (11)$$

where N is the number of executed runs, and $N = 20$. OF_i denotes the value of the OF obtained in the i th run.

B. Sensitivity Study of Parameters

This subsection will conduct a sensitivity study on different parameters:

- F , which affects collaborative solutions and evolutionary trends.
- F_CR , which controls the degree of crossover.
- Ex_count , which indicates the size of ϑ .
- $count_1$, which selects the execution stage in the *three-stage adaptive collaboration strategy*.
- $count_2$, which determines the execution of *DE/target-to-minimum boundary best*.
- The random factor R , which helps to choose the *DE/target-to-perturbed best/1* or *2*.

Fig. 5 shows the variation trend of each parameter. Based on the results, we ultimately choose: $F = 0.4$ (meaning that F_1 , F_2 , and F_3 are set to 0.4), $F_CR = 0.5$, $R = 0.4$, $Ex_count = 2$, $count_1 = 6$, and $count_2 = 7$. As shown in Fig. 5, too large or too small F and R will lead to the degradation of the algorithm's performance. The OF value gradually increases with respect to Ex_count . This indicates that there is no need for too many historical solutions. The reason may be that storing too many solutions might lead to the wrong evolutionary direction of the current solution, thereby hampering the performance of the strategy. For other parameters, F_CR , $count_1$, and $count_2$, the variation of OF values is irregular. However, in terms of the variation, the settings of these parameters also affect the performance of SADEA.

C. The effectiveness of the proposed strategies

To investigate the impact of the proposed strategies, ablation experiments are conducted in this section. We use the following abbreviations to distinguish between variants of SADEA: *V-bound* represents that there is no *boundary randomization stage* ('V' means 'variant', '-' means 'remove'). *V-Histor* and *V-Re* indicate the absence of *knowledge-assisted collaboration* and *range restructuration* stages, respectively. *V-DE1*, *V-DE2*, and *V-DE3* mean that the designed DE strategies (*DE/target-to-minimum boundary best*, *DE/target-to-disturbed best/1* and *2*) are not used, respectively. SADEA contains all the strategies. The results are given in Table II and Fig. 6. Note that, in Table II, bold font means that the corresponding algorithm obtains the best OF or RI values among all the algorithms.

As shown in Table II, SADEA obtains 10 out of 20 best values, larger than the numbers of the best OF s obtained by *V-bound* (0/20), *V-Histor* (4/20), *V-Re* (3/20), *V-DE1* (1/20), *V-DE2* (1/20), and *V-DE3* (2/20). Moreover, SADEA achieves the smallest RI value. The results imply that the proposed strategies are effective in improving the performance of SADEA. Fig. 6 gives a violin chart drawn based on the numeric results in Table II. In addition to showing the statistics, the advantage of using a violin is that it clearly illustrates the overall

TABLE II
PERFORMANCE COMPARISONS (REGARDING OF AND RI) BETWEEN THE VARIANTS WHERE ONE OF THE PROPOSED STRATEGIES IS REMOVED

Row	V-Bound	V-His	V-Re	V-DE1	V-DE2	V-DE3	SADEA
Run 1	95865	40427	41604	44884	46134	41440	41509
Run 2	82323	42446	68288	45190	45829	40033	40648
Run 3	100560	45892	41541	42049	48037	45362	42604
Run 4	94768	42439	62568	43743	61084	40024	39594
Run 5	97227	40680	41236	48341	61473	40092	40499
Run 6	132880	40814	41021	45859	42649	42883	48874
Run 7	109590	41867	40777	40937	41953	43784	39992
Run 8	71319	41922	42389	42999	43176	41606	40817
Run 9	101830	47500	41309	43775	42688	43530	40397
Run 10	91169	41932	48536	43560	41202	48916	40843
Run 11	124160	40579	44964	41584	77525	41566	40871
Run 12	103790	42401	43293	45196	50325	42313	40755
Run 13	112420	42609	41250	42778	61731	50030	43279
Run 14	92270	41925	45893	46448	44478	42334	40706
Run 15	121320	39956	41614	42187	48458	40489	39814
Run 16	111640	42781	54542	45930	41653	41942	41653
Run 17	60621	51841	41635	40983	51892	42433	42002
Run 18	78216	41565	40615	43851	40507	52277	40308
Run 19	113530	41094	41454	43819	61680	43547	41307
Run 20	92634	40773	40407	42988	44428	42117	48459
RI	99407	42572	45247	43855	49845	43336	41747

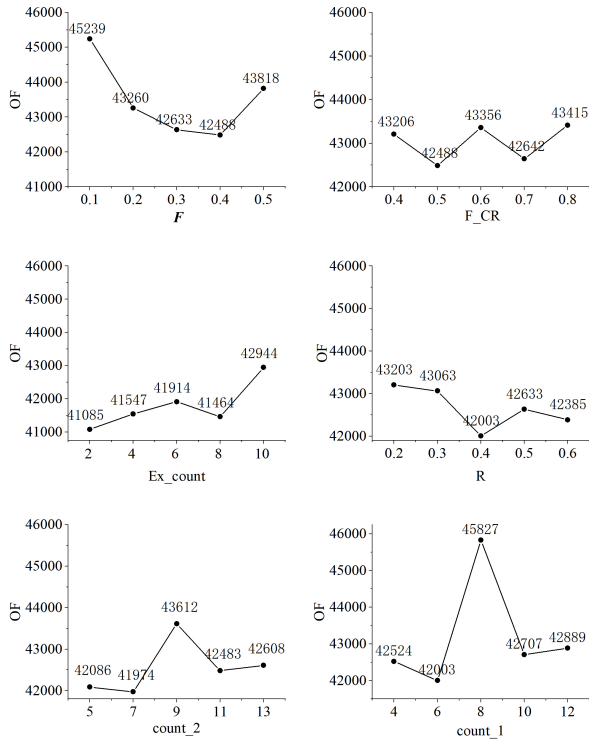


Fig. 5. The trend of OF with respect to different parameters

distribution of OFs. In Fig. 6, the black bar in the center of the violin indicates the interquartile range, and the white dots denote the median OF values. It shows that the black bars and white dots in SADEA's violin are the lowest amongst all the variants, indicating that SADEA outperforms all the variants. From the size of violins, it can be inferred that the *boundary randomization* has the greatest impact on the algorithm. Indeed, after removing this strategy, the corresponding

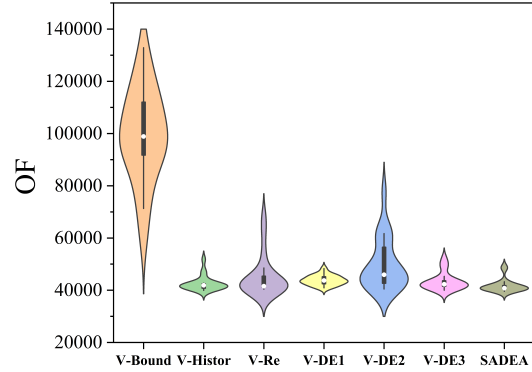


Fig. 6. Violin chart for comparison of different variants

variant has the worst OF values. In addition, *range restructuration* and *DE/target-to-disturbed best/2* have a large impact on the performance of SADEA. After removing these two strategies, the search ability of SADEA becomes poor, resulting in unstable OF values. Thus, it is necessary to use strategies with strong perturbation ability, *range restructuration* and *DE/target-to-perturbed best/2* precisely to meet this requirement. For other strategies, they have a relatively small impact on SADEA. As can be seen from the Table II and Fig. 6, if these strategies are removed, the search performance of SADEA decreases to a certain degree.

D. The Performance Comparison of All Algorithms

This subsection compares SADEA with the state-of-the-art algorithms for solving ERM problems: HyDE [12], CUMDANCauchy, CCSTG, Presto, HC2RCEDUMDA, and ReSaDE, which participated in the 2020, 2021, and 2022 competitions on evolutionary computation in the energy domain: smart grid scheduling applications. Among them, CUMDANCauchy, CCSTG, and ReSaDE won the first place in 2020, 2021, and 2022 competitions, respectively. The proposed SADEA adopts the parameters tuned in Subsection VI.B, while other

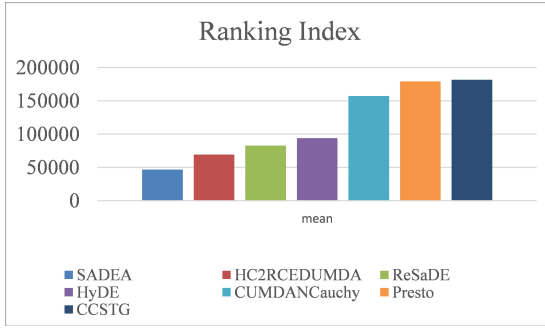


Fig. 7. Ranking index for SADEA and peer algorithms when $G = 3,000$

algorithms use the parameters suggested by their developers. Tables III and IV list the OF values obtained by all algorithms in 20 independent runs. Like in Table II, the best OF and RI values are highlighted in bold. As shown in Tables III and IV, SADEA achieves the best results in all the runs, showing clearly its superiority over the peer algorithms.

To demonstrate the differences between these algorithms, we plotted the RI values, min/max OF values, and accumulated OF values in Figs. 7, 8, and 9 ($G = 3,000$) and Figs. 10, 11, and 12 ($G = 5,000$). The RI values (Figs. 7 and 10) are drawn in ascending order according to Tables III and IV. Each color rectangle indicates an algorithm. These plots provide an intuitive comparison of the overall performance of the algorithms. From these plots, it can be seen that SADEA has the best performance. The min/max values, as shown in Figs. 8 and 11, are drawn based on the minimum and maximum values in Tables III and IV. These two graphs reflect the fluctuation of OF values in all runs. It can be seen that although SADEA has the largest fluctuation, it still obtains smaller min/max values than the peer algorithms. The max value of the SADEA is smaller than the min value of the second-best algorithm HC2RCEDUMDA. In addition, Figs. 9 and 12 give the accumulated OF values for SADEA and peer algorithms. It can be seen from these figures, SADEA achieves the minimum OF values and saves a significant amount of costs. Comparing Figs. 13 and 14, we can find that the solutions obtained by SADEA get more centralized when G is increased from 3,000 to 5,000, while solutions of other algorithms have small changes. It indicates that SADEA can continuously evolve, while other algorithms may fall into local optimum. From the overall perspective of the box plots, the OF values of SADEA are lower than other algorithms, further demonstrating the effectiveness of SADEA.

The reason for the good performance of SADEA may be that *boundary randomization* and *range restructuration* effectively enhance the algorithm's global search ability. *knowledge-assisted collaboration* saves historical solutions and uses them to explore promising solutions in neighborhoods. This strategy aims at improving the diversity of solutions while stabilizing the local search ability. However, SADEA focuses its attention on a solution, which inevitably leads to more 'precise' evolution of the solution. It will lead to an issue: if the perturbation ability of SADEA is not strong, it is likely to fall into the local optimum. Therefore, it is necessary to design strategies with strong perturbation to improve the global search ability of SADEA, helping the solution jump out of the local optimum. The proposed DE strategies, combined with the *three-stage adaptive collaboration strategy*, achieve the desired goal. They overcome the shortcomings of traditional strategies in local search abilities. Furthermore, as demonstrated in Section VI-C, the proposed *boundary randomization* greatly improves the search ability of SADEA.

E. Statistical Validation and Convergence Curves

In this subsection, to check whether there exist significant differences between SADEA and peer algorithms, we performed statistical

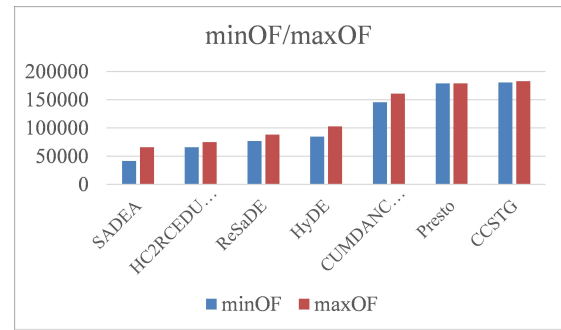


Fig. 8. minOF/maxOF values for SADEA and peer algorithms when $G = 3,000$

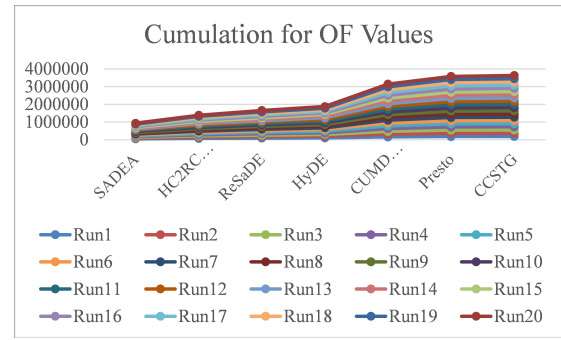


Fig. 9. Accumulated OF values for SADEA and peer algorithms when $G = 3,000$

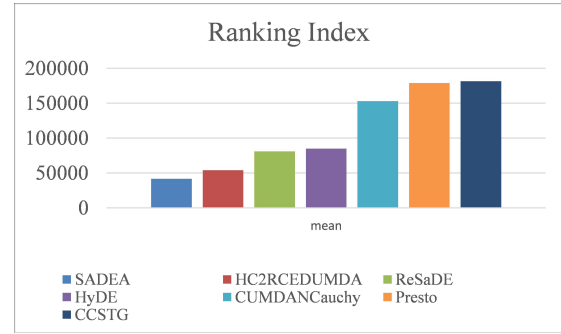


Fig. 10. Ranking index for SADEA and peer algorithms when $G = 5,000$

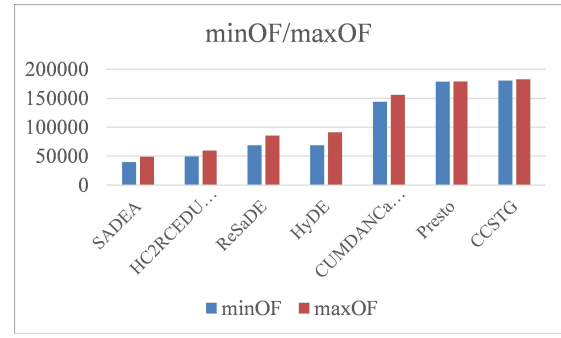


Fig. 11. minOF/maxOF values for SADEA and peer algorithms when $G = 5,000$

TABLE III
PERFORMANCE COMPARISONS (REGARDING OF AND RI) BETWEEN THE PEER ALGORITHMS WHEN $G = 3,000$

Row	SADEA	HC2RCEDUMDA	ReSaDE	HyDE	CUMDANCauchy	Presto	CCSTG
Run 1	47771	72517	88159	101260	156100	178850	182710
Run 2	41648	66596	82663	94049	154800	178890	180750
Run 3	44239	69077	78367	97599	157740	178880	180770
Run 4	48659	66590	87895	87998	157680	178900	180830
Run 5	42024	65801	79883	98952	149990	178880	182090
Run 6	42190	74884	81738	99533	159350	178880	180630
Run 7	44115	68452	85055	91380	160650	178910	181270
Run 8	44561	67257	79195	94551	160690	178930	182290
Run 9	42541	70743	81151	91445	157740	178920	180900
Run 10	65734	68911	83439	98171	145450	178890	182140
Run 11	48271	68420	80783	87865	157790	178910	181270
Run 12	43324	66628	84231	102680	157520	178890	180530
Run 13	42568	73408	81357	98085	156100	178870	181350
Run 14	42446	65954	78773	90092	155070	178850	181190
Run 15	42059	67907	76726	93571	160720	178900	181500
Run 16	51161	73224	86613	84695	160170	178910	182090
Run 17	42817	69812	80934	84690	158380	178930	181400
Run 18	48806	67911	80608	86338	159340	178860	180870
Run 19	51921	70281	86703	92194	157190	178960	181910
Run 20	56333	67198	88030	100880	159660	178910	182350
RI	46659	69079	82615	93801	157110	178900	181440

TABLE IV
PERFORMANCE COMPARISONS (REGARDING OF AND RI) BETWEEN THE PEER ALGORITHMS WHEN $G = 5,000$

Row	SADEA	HC2RCEDUMDA	ReSaDE	HyDE	CUMDANCauchy	Presto	CCSTG
Run 1	41509	56722	81563	88676	152430	178760	182710
Run 2	40648	52413	85619	68679	154810	178750	180750
Run 3	42604	57521	79784	90745	152850	178750	180770
Run 4	39594	49503	82439	78569	153180	178760	180830
Run 5	40499	52351	83220	87263	154990	178740	182090
Run 6	48874	59645	80071	85397	153940	178730	180630
Run 7	39992	51477	74485	87365	155330	178750	181270
Run 8	40817	52670	83258	91225	152840	178730	182290
Run 9	40397	56896	79594	89380	153110	178760	180900
Run 10	40843	53481	80655	89126	151420	178730	182140
Run 11	40871	52927	84101	79512	156020	178720	181270
Run 12	40755	55993	80059	84183	153710	178770	180530
Run 13	43279	55064	68860	91198	155930	178770	181340
Run 14	40706	51754	80087	78894	155750	178740	181190
Run 15	39814	53854	76660	79179	143770	178720	181500
Run 16	41653	54845	80593	86023	153670	178770	182090
Run 17	42002	52120	84121	83458	148390	178790	181400
Run 18	40308	54500	85601	80524	153630	178730	180870
Run 19	41307	55376	85037	91209	155200	178730	181910
Run 20	48459	52775	82475	84846	148890	178760	182350
RI	41747	54094	80914	84773	152990	178750	181440

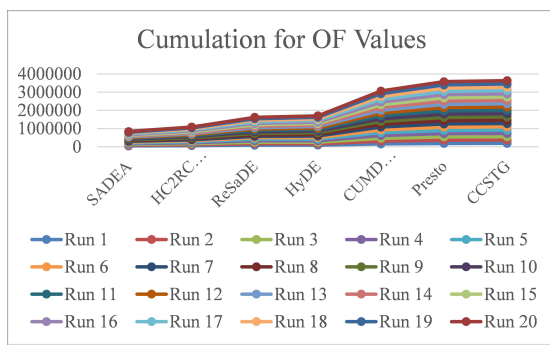


Fig. 12. Accumulated OF values for SADEA and peer algorithms when $G = 5,000$

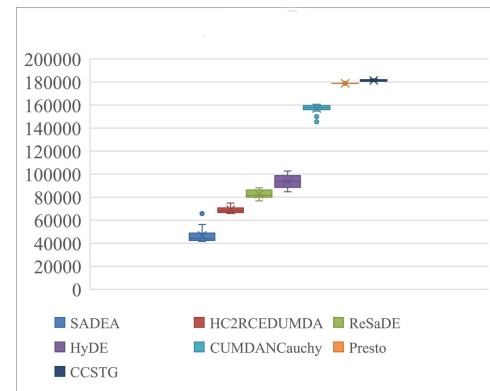


Fig. 13. Box plots for SADEA and the peer algorithms when $G = 3,000$

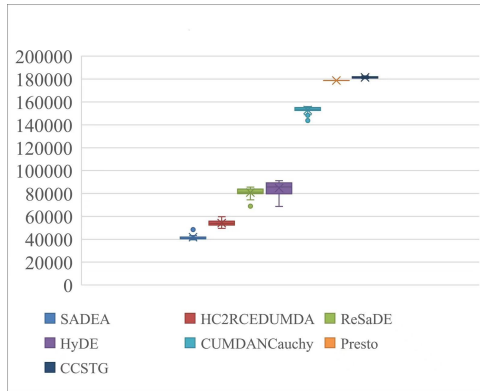


Fig. 14. Box plots for SADEA and peer algorithms when $G = 5,000$

tests with the Wilcoxon test. Tables V and VI list the Wilcoxon test when $G = 3000$ and 5000 , respectively. R+ represents the sum of the OF values that are higher than SADEA compared to peer algorithms. R- represents the sum of the OF values that are less in SADEA compared to peer algorithms. The p-value represents the degree of significant difference between the two algorithms. If p-value < 0.05 , the hypothesis is rejected, indicating a significant difference between SADEA and peer algorithms. Conversely, there is no significant difference. According to the results in Tables V and VI, all p-values < 0.05 , thus the hypotheses are rejected. All R- values obtained are very large, while R+ values are 0, this shows that the proposed SADEA algorithm performs significantly better than the other algorithms. To summarize, the results indicate that there are significant differences between SADEA and peer algorithms.

TABLE V

RESULTS OF THE WILCOXON TEST FOR PAIRWISE COMPARISONS BETWEEN SADEA AND EACH PEER ALGORITHM (WHEN $G = 3,000$)

Wilcoxon test	R+	R-	p-value	Hypothesis
SADEA vs HC2RCEDUMDA	0	448383	1.15E-17	Reject
SADEA vs ReSaDE	0	719115	6.91E-24	Reject
SADEA vs HYDE	0	942840	2.06E-25	Reject
SADEA vs CUMDANCauchy	0	2208942	1.3E-41	Reject
SADEA vs Presto	0	2644732	3.3E-47	Reject
SADEA vs CCSTG	0	2695652	2E-47	Reject

TABLE VI

RESULTS OF THE WILCOXON TEST FOR PAIRWISE COMPARISONS BETWEEN SADEA AND EACH PEER ALGORITHM (WHEN $G = 5,000$)

Wilcoxon test	R+	R-	p-value	Hypothesis
SADEA vs HC2RCEDUMDA	0	246956	3.32E-18	Reject
SADEA vs ReSaDE	0	783351	2.41E-31	Reject
SADEA vs HYDE	0	860520	2.98E-28	Reject
SADEA vs CUMDANCauchy	0	2224929	1.61E-51	Reject
SADEA vs Presto	0	2740029	3.48E-62	Reject
SADEA vs CCSTG	0	2793899	5.76E-62	Reject

Subsequently, to check the convergence of each algorithm, we select 12 runs and then draw their curves to verify the convergence performance. When $G = 3,000$, we randomly chose the run numbers: 2, 5, 9, 12, 15, and 17. When $G = 5,000$, we randomly chose the run numbers: 1, 4, 7, 11, 14, and 18. As shown in Figs. 15 and 16, the second best algorithm, HC2RCEDUMDA, falls into a local optimum in later evolutions. Other peer algorithms, such as ReSaDE and HyDE, are not as strong as SADEA, though they do not fall into local optimum in most cases. CUMDANCauchy is often trapped in local optimum, and occasionally jumps out of this state. However, from the convergence trend, the overall performance of this algorithm

is not strong. Presto and CCSTG are trapped in a local optimum from the beginning of their execution and are unable to jump out of it. Compared with the above algorithms, SADEA can converge to a steady and better OF value more quickly. Overall, it exhibits a continuous evolution, albeit with a slower speed in later stages. The above convergence curves further confirm that SADEA outperforms other peer algorithms in improving the convergence. In summary, the proposed algorithm is effective for solving the ERM problem under uncertainty.

VII. CONCLUSION AND FUTURE WORK

In this paper, a self-adaptive collaborative differential evolution algorithm, named SADEA, is proposed to solve the ERM problem under uncertainty. In SADEA, a *three-stage adaptive collaboration strategy* is designed to generate different collaborative solutions to help the evolution of the current solution. In *boundary randomization*, collaborative solutions are generated to perturb the current solution. In the *knowledge-assisted collaboration*, the collaborative solutions are generated using historical archive, whose purpose is to help improve the global and local search abilities of SADEA. In addition, three different DE strategies are proposed to reduce the costs of aggregators in the ERM problem. The generated superior solutions directly participate in the next collaboration after *boundary control and elite selection*. In the experiments, sensitivity study and analysis of parameters are conducted. Then, the effectiveness of all proposed strategies is verified. Next, to verify the stability of the algorithm, SADEA is compared with six peer algorithms. The results demonstrate that SADEA outperforms peer algorithms in terms of solutions' diversity and convergence.

We found that single-individual mechanism is useful for solving the continuous optimization problem, especially the ERM problem addressed in this paper. In addition, based on the single-individual mechanism, the performance of the algorithm can be further enhanced by using strategies that can improve the global search ability. Last but not the least, to maintain a balance between global and local search abilities, it is effective to use a multi-stage adaptive collaboration framework.

In the future, we will consider further optimizing the structure of SADEA, and will reduce the number of parameters with fixed settings. Moreover, there is value in improving the local and global search abilities of the algorithm, particularly in the late evolution stage. Also, it is interesting to incorporate micro search [46], neural networks [47], or reinforcement learning [48] into the EA algorithms. Finally, it is possible to make use of the advantages of other EA algorithms, e.g., Discrete Bee Colony Optimization Algorithms [49] and Meme algorithms [50].

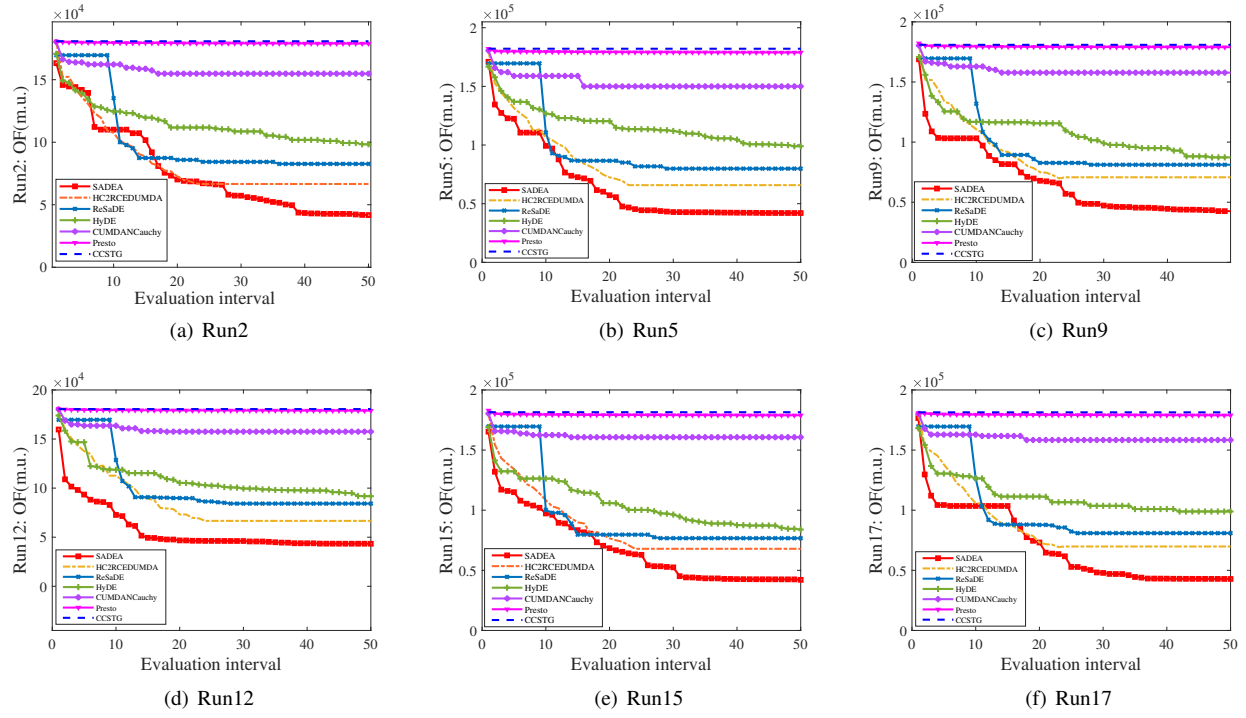


Fig. 15. Convergence curves of SADEA and peer algorithms when $G = 3,000$

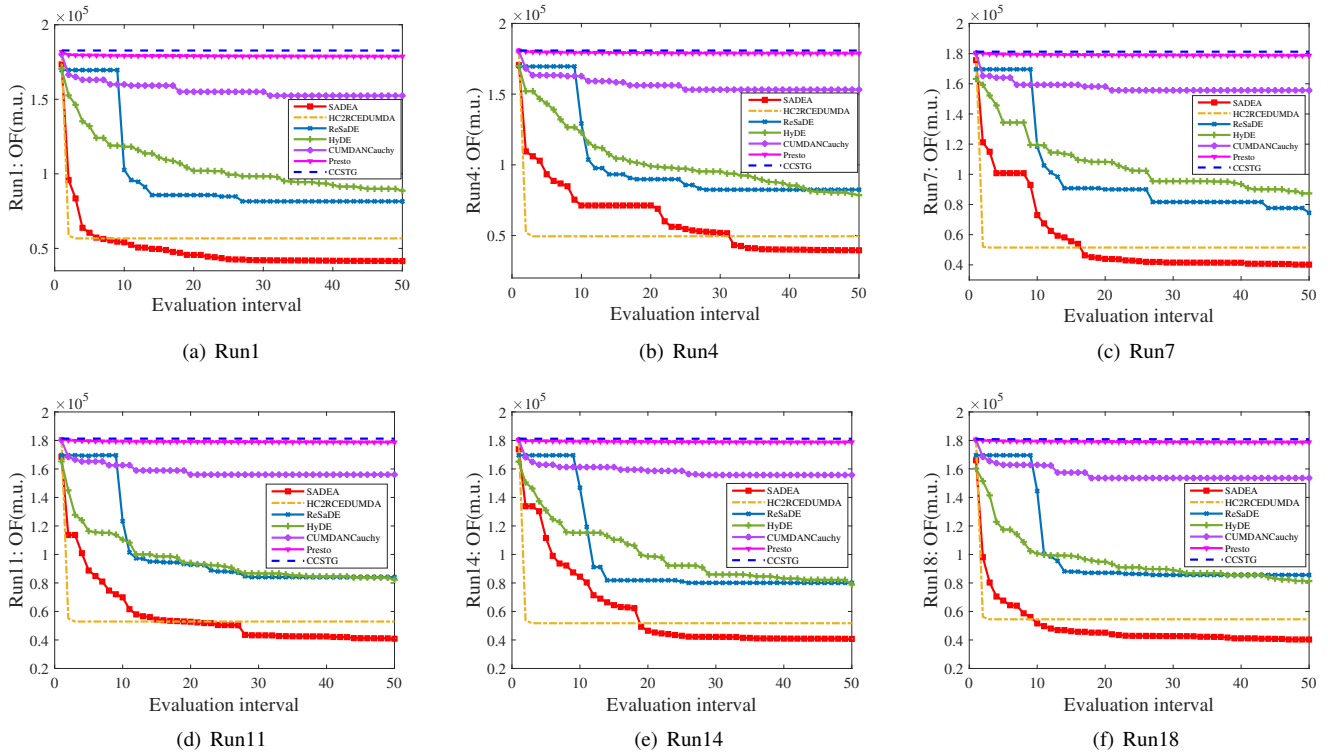


Fig. 16. Convergence curves of SADEA and peer algorithms when $G = 5,000$

REFERENCES

- [1] Y. Yan, Y. Qian, H. Sharif, and D. Tipper, "A survey on smart grid communication infrastructures: Motivations, requirements and challenges," *IEEE Communications Surveys & Tutorials*, vol. 15, no. 1, pp. 5–20, 2013.
- [2] F. Lezama, L. E. Sucar, E. D. Cote, J. Soares, and Z. Vale, "Differential evolution strategies for large-scale energy resource management in smart grids," in *Genetic & Evolutionary Computation Conference Companion*, 2017, pp. 1279–1286.
- [3] J. Soares, B. Canizes, M. Ghazvini, Z. Vale, and G. K. Venayagamoorthy, "Two-stage stochastic model using benders' decomposition for large-scale energy resources management in smart grids," *IEEE Transactions on Industry Applications*, vol. PP, no. 6, pp. 1–1, 2017.
- [4] L. Fernando, S. Joao, H. L. Pablo, K. Michael, P. Tiago, and A. Maria, "Local energy markets: Paving the path towards fully transactive energy systems," *IEEE Transactions on Power Systems*, vol. PP, pp. 1–1, 2018.
- [5] J. Soares, M. A. Fotouhi, M. Silva, and Z. Vale, "Multi-dimensional signaling method for population-based metaheuristics: Solving the large-scale scheduling problem in smart grids," *Swarm & Evolutionary Computation*, pp. 13–32, 2016.
- [6] T. Logenthiran, D. Srinivasan, and Z. S. Tan, "Demand side management in smart grid using heuristic optimization," *IEEE Transactions on Smart Grid*, vol. 3, no. 3, pp. 1244–1252, 2012.
- [7] A. Trivedi, D. Srinivasan, S. Biswas, and T. Reindl, "A genetic algorithm – differential evolution based hybrid framework: Case study on unit commitment scheduling problem," *Information Sciences*, pp. 275–300, 2016.
- [8] M. Rahimian and L. Baringo, "Strategic bidding for a virtual power plant in the day-ahead and real-time markets: A price-taker robust optimization approach," *IEEE Transactions on Power Systems*, vol. 31, no. 4, pp. 2676–2687, 2016.
- [9] LW. Tan, ZF. Yuan, JY. QK, HH. Dong, and FG. "A bi-level stochastic scheduling optimization model for a virtual power plant connected to a wind-photovoltaic-energy storage system considering the uncertainty and demand response," *APPL ENERG*, vol. 2016,171, no. -, pp. 184–199, 2016.
- [10] W. Su, J. Wang, and J. Roh, "Stochastic energy scheduling in microgrids with intermittent renewable energy resources," *IEEE Transactions on Smart Grid*, vol. 5, no. 4, 2013.
- [11] H. Liang and W. Zhuang, "Stochastic modeling and optimization in a microgrid: A survey," *Energies*, vol. 7, no. 4, pp. 2027–2050, 2014.
- [12] F. Lezama, J. Soares, R. Faia, T. Pinto, and Z. Vale, "A new hybrid-adaptive differential evolution for a smart grid application under uncertainty," in *2018 IEEE Congress on Evolutionary Computation (CEC)*, 2018.
- [13] Z. Wan, G. Wang, and B. Sun, "A hybrid intelligent algorithm by combining particle swarm optimization with chaos searching technique for solving nonlinear bilevel programming problems," *Swarm & Evolutionary Computation*, vol. 8, no. Complete, pp. 26–32, 2013.
- [14] D. E. Goldberg, "Genetic algorithms in search, optimization, and machine learning," Addison-Wesley Pub. Co., 1989.
- [15] J. J. Grefenstette, "Grefenstette, j.j.: Optimization of control parameters for genetic algorithms. ieee trans. syst. man cybern. 16(1), 122-128," *IEEE Transactions on Systems Man and Cybernetics*, vol. 16, no. 1, pp. 122–128, 1986.
- [16] J. Brest, S. Greiner, B. Boskovic, M. Mernik, and V. Zumer, "Self-adapting control parameters in differential evolution: A comparative study on numerical benchmark problems," *IEEE Transactions on Evolutionary Computation*, vol. 10, no. 6, pp. 646–657, 2006.
- [17] C. Coello, G. T. Pulido, and M. S. Lechuga, "Handling multiple objectives with particle swarm optimization," *IEEE Transactions on Evolutionary Computation*, vol. 8, no. 3, pp. 256–279, 2004.
- [18] R. Ruiz and T. Stützle, "A simple and effective iterated greedy algorithm for the permutation flowshop scheduling problem," *European Journal of Operational Research*, vol. 177, no. 3, pp. 2033–2049, 2007.
- [19] H. X. Qin, Y. Y. Han, B. Zhang, L. L. Meng, Y. P. Liu, Q. K. Pan, and D. W. Gong, "An improved iterated greedy algorithm for the energy-efficient blocking hybrid flow shop scheduling problem," *Swarm and Evolutionary Computation*, no. 69-, p. 69, 2022.
- [20] Y. H. Wang, Y. Y. Han, Y. T. Wang, M. F. Tasgetiren, J. Q. Li, and K. Z. Gao, "Intelligent optimization under the makespan constraint: Rapid evaluation mechanisms based on the critical machine for the distributed flowshop group scheduling problem," *European Journal of Operational Research*, 2023.
- [21] H. Qin, Y. Han, Y. Wang, Y. Liu, J. Li, and Q. Pan, "Intelligent optimization under blocking constraints: A novel iterated greedy algorithm for the hybrid flow shop group scheduling problem," *Knowledge-Based Systems*, vol. 258, p. 109962, 2022.
- [22] J. Q. Li, Y. Du, K. Z. Gao, P. Y. Duan, and P. N. Suganthan, "A hybrid iterated greedy algorithm for a crane transportation flexible job shop problem," *IEEE Transactions on Automation Science and Engineering*, vol. PP, no. 99, pp. 1–18, 2021.
- [23] F. Lezama, J. Soares, B. Canizes, Z. Vale, and R. Romero, "Call for competition on evolutionary computation in the energy domain: Smart grid applications 2021," 2021. [Online]. Available: <http://www.gecad.isept.ipp.pt/ERM-competitions/2021-2/>
- [24] J. Soares, F. Lezama, J. Almeida, B. Canizes, and Z. Vale, "Call for competition on evolutionary computation in the energy domain: Risk-based energy scheduling 2022," in <http://www.gecad.isept.ipp.pt/ERM-competitions/2022-2/>, 2022.
- [25] J. Soares, F. Lezama, Z. Vale, and K. Venayagamoorthy, "2023 call for special session cec-evolutionary algorithms for complex optimization in the energy domain," 2023. [Online]. Available: <http://www.gecad.isept.ipp.pt/ERM-competitions/ss2023/>
- [26] X. Cao, J. Wang, J. Wang, and B. Zeng, "A risk-averse conic model for networked microgrids planning with reconfiguration and reorganizations," *IEEE Transactions on Smart Grid*, vol. PP, no. 99, 2019.
- [27] A. Khodaei, "Resiliency-oriented microgrid optimal scheduling," *IEEE Transactions on Smart Grid*, vol. 5, no. 4, pp. 1584–1591, 2014.
- [28] L. Che and M. Shahidehpour, "Dc microgrids: Economic operation and enhancement of resilience by hierarchical control," *IEEE Transactions on Smart Grid*, vol. 5, no. 5, pp. 2517–2526, 2014.
- [29] D. N. Trakas, M. Panteli, N. D. Hatziargyriou, and P. Mancarella, "Spatial risk analysis of power systems resilience during extreme events," *Risk Analysis*, vol. 39, no. 1, pp. 195–211, 2019.
- [30] H. Saber, M. Moeini-Aghaie, M. Ehsan, and M. Fotuhi-Firuzabad, "A scenario-based planning framework for energy storage systems with the main goal of mitigating wind curtailment issue," *International Journal of Electrical Power & Energy Systems*, vol. 104, no. JAN., pp. 414–422, 2019.
- [31] O. Cavus, A. S. Kocaman, and O. Yilmaz, "A risk-averse approach for the planning of a hybrid energy system with conventional hydropower," *Computers & operations research*, no. Feb., p. 126, 2021.
- [32] F. S. Gazijahani and J. Salehi, "Optimal bi-level model for stochastic risk-based planning of microgrids under uncertainty," *IEEE Transactions on Industrial Informatics*, pp. 1–1, 2017.
- [33] L. Guo, T. Sriyakul, S. Nojavan, and K. Jermsittiparsert, "Risk-based traded demand response between consumers' aggregator and retailer using downside risk constraints technique," *IEEE Access*, vol. PP, no. 99, pp. 1–1, 2020.
- [34] M. Tavakoli, F. Shokrdehaki, M. F. Akorede, M. Marzband, I. Vechiu, and E. Pouresmaeil, "Cvar-based energy management scheme for optimal resilience and operational cost in commercial building microgrids," *International Journal of Electrical Power & Energy Systems*, vol. 100, no. SEP., pp. 1–9, 2018.
- [35] J. Almeida, J. Soares, F. Lezama, and Z. Vale, "Robust energy resource management incorporating risk analysis using conditional value-at-risk," *IEEE Access*, vol. 10, pp. 16 063–16 077, 2022.
- [36] B. Mla, D. Rgc, A. Jm, A. Mb, and E. Fl, "Cellular estimation of distribution algorithm designed to solve the energy resource management problem under uncertainty - sciencedirect," *Engineering Applications of Artificial Intelligence*, vol. 101.
- [37] K. E. Parsopoulos and M. N. Vrahatis, *UPSO: A Unified Particle Swarm Optimization Scheme*. International Conference of Computational Methods in Sciences and Engineering 2004 (ICCMSE 2004), 2019.
- [38] J. Garcia-Guarin, D. Alvarez, A. Bretas, and S. Rivera, "Schedule optimization in a smart microgrid considering demand response constraints," *Energies*, vol. 13, no. 1, p. 4567, 2020.
- [39] D. Dabhi and K. Pandya, "Uncertain scenario based microgrid optimization via hybrid levy particle swarm variable neighborhood search optimization (hlpsvnso)," *IEEE Access*, vol. PP, no. 99, pp. 1–1, 2020.
- [40] F. Lezama, J. Soares, Z. Vale, J. Rueda, S. Rivera, and I. Elrich, "2017 ieee competition on modern heuristic optimizers for smart grid operation: Testbeds and results," *Swarm and Evolutionary Computation*, 2019.
- [41] N. Grawe-Kuska, H. Heitsch, and W. Romisch, "Scenario reduction and scenario tree construction for power management problem," in *Power Tech Conference Proceedings, 2003 IEEE Bologna*, 2003.
- [42] B. Canizes, J. Soares, Z. Vale, and J. Corchado, "Optimal distribution grid operation using dlmp-based pricing for electric vehicle charging infrastructure in a smart city," *Energies*, vol. 12, no. 4, 2019.

- [43] X. Han, Y. Han, B. Zhang, H. Qin, J. Li, Y. Liu, and D. Gong, "An effective iterative greedy algorithm for distributed blocking flowshop scheduling problem with balanced energy costs criterion," *Applied Soft Computing*, vol. 129, p. 109502, 2022.
- [44] J. P. Huang, Q. K. Pan, Z. H. Miao, and L. Gao, "Effective constructive heuristics and discrete bee colony optimization for distributed flowshop with setup times," *Engineering Applications of Artificial Intelligence*, vol. 97, p. 104016, 2021.
- [45] V. Miranda and N. Fonseca, "Epsso-evolutionary particle swarm optimization, a new algorithm with applications in power systems," 2002, pp. 745–750.
- [46] H. Huang, S. L. Yang, X. Q. Li, and Z. F. Hao, "An embedded hamiltonian graph-guided heuristic algorithm for two-echelon vehicle routing problem," *IEEE Transactions on Cybernetics*, vol. 52, no. 7, pp. 5695–5707, 2022.
- [47] J. P. Huang, L. Gao, X. Y. Li, and C. J. Zhang, "A novel priority dispatch rule generation method based on graph neural network and reinforcement learning for distributed job-shop scheduling," *Journal of Manufacturing Systems*, vol. 69, pp. 119–134, 2023.
- [48] H. X. Qin, Y. Y. Han, Q. D. Chen, L. Wang, Y. T. Wang, J. Q. Li, and Y. P. Liu, "Energy-efficient iterative greedy algorithm for the distributed hybrid flow shop scheduling with blocking constraints," *IEEE Transactions on Emerging Topics in Computational Intelligence*, pp. 1–16, 2023.
- [49] J. P. Huang, Q. K. Pan, Z. H. Miao, and L. Gao, "Effective constructive heuristics and discrete bee colony optimization for distributed flowshop with setup times," *Engineering Applications of Artificial Intelligence*, vol. 97, p. 104016, 2021.
- [50] J. J. Wang and L. Wang, "A bi-population cooperative memetic algorithm for distributed hybrid flow-shop scheduling," *IEEE Transactions on Emerging Topics in Computational Intelligence*, vol. PP, no. 99, pp. 1–15, 2020.



Yi Xiang received the B.Sc. and M.Sc. degrees in mathematics from Guangzhou University, Guangzhou, China, in 2010 and 2013, respectively, and the Ph.D. degree in computer science from Sun Yat-sen University, Guangzhou, in 2018. He is currently an associate professor within the School of Software Engineering, South China University of Technology, Guangzhou. His current research interests include software product lines, search-based software engineering, and multi-objective optimization.



Fangqing Liu received the B.E. degree and Ph.D degree in software engineering from South China University of Technology, Guangzhou, China, in 2016 and 2021 respectively. He is currently a post-doctor in software engineering at School of Software Engineering, South China University of technology, Guangzhou, China. His current research interests in AIGC including applications in automated software test case generation and image data augmentation.



Haoxiang Qin received B.S. and M.S. degrees from the School of Computer Science, Liaocheng University, Shandong, China. He is currently pursuing the Ph.D. degree in software engineering at School of Software Engineering, South China University of Technology, Guangzhou, China.

His current research interests include intelligent optimization algorithms and their applications, such as hybrid flow shop scheduling, flexible job-shop scheduling, and electric system scheduling.



shop scheduling.

Yuyan Han received the M.S. degree from the School of Computer Science, Liaocheng University, Liaocheng, China, in 2012, and the Ph.D. degree in control theory and control engineering from the China University of Mining and Technology, Xuzhou, China, in 2016.

Since 2016, she has been a associate professor with the School of Computer Science, Liaocheng University. She has authored over 30 refereed papers. Her current research interests include evolutionary computation, multiobjective optimization, and flow-



Wenlei Bai (M'15) received the B.S. degree in Electrical Engineering in 2009 from Southwest University for Nationalities, M.S. degree in Engineering Technology in 2011 from West Texas A&M University, and Ph. D. degree in Electrical and Computer Engineering in 2017 from Baylor University. He is currently a principal application developer at Oracle Energy and Water to conduct research and development on advanced distribution management system.

His research interests include power system planning and operation, electricity market, supply chain optimization, computational intelligence, and their applications to power systems, and modeling, simulation, and control of micro-grids with renewable and distributed energy sources.



Ling Wang received the B.Sc. in automation and Ph.D. degrees in control theory and control engineering from Tsinghua University, Beijing, China, in 1995 and 1999, respectively.

Since 1999, he has been with the Department of Automation, Tsinghua University, where he became a full professor in 2008. His current research interests include intelligent optimization and production scheduling. He has authored five academic books and more than 260 refereed papers.

Professor Wang is a recipient of the National Natural Science Fund for Distinguished Young Scholars of China, the National Natural Science Award (Second Place) in 2014, the Science and Technology Award of Beijing City in 2008, the Natural Science Award (First Place in 2003, and Second Place in 2007) nominated by the Ministry of Education of China. Professor Wang now is the Editor-in-Chief of International Journal of Automation and Control, and the Associate Editor of IEEE Transactions on Evolutionary Computation.